

## Articles

# A Continuous-Flow System for High-Precision Kinetics Using Small Volumes

Xianzhi Zhou,<sup>†</sup> Rohit Medhekar,<sup>‡</sup> and Michael D. Toney\*

Department of Chemistry, University of California–Davis, One Shields Avenue, Davis, California 95616

**A generally applicable continuous-flow kinetic analysis system that gives data of a precision high enough to measure small kinetic isotope effects for enzymatic and nonenzymatic reactions is described. It employs commercially available components that are readily assembled into an apparatus that is easy to use. It operates under laminar flow conditions, which requires that the time between the initiation of the reaction in the mixer and the observation be long enough that molecular diffusion can effect a symmetrization of the concentration profile that results from a thin plug of reagents introduced at the mixer. The analysis of a second-order irreversible reaction under pseudo-first-order conditions is presented. The *Yersinia pestis* protein tyrosine phosphatase catalyzed hydrolysis of *p*-nitrophenyl phosphate is characterized with the system, and a proton inventory on  $k_{\text{cat}}$  is presented.**

Steady-state spectrophotometric enzyme kinetic assays are typically performed by mixing solutions that differ in substrate concentration in several cuvettes and observing the initial rates of the individual reactions in a spectrophotometer. Nonlinear regression analysis of the initial rate data typically yields kinetic parameters that have errors of 5–20%. This is generally acceptable for many routine kinetic analyses, but some require much higher precision. Kinetic isotope effect (KIE) measurements are a good example. Primary deuterium KIEs are generally large enough (e.g., 2–6-fold) that kinetic measurements using manual techniques define them sufficiently well. On the other hand, secondary deuterium and heavy atom KIEs pose greater challenges that cannot generally be met by manual techniques. Rosenberg and Kirsch have shown that with extreme care, these challenges are not insurmountable.<sup>1</sup> The development of a general purpose, easy to use instrument capable of measuring kinetics with high precision would be a welcome addition to the armamentarium of the biochemist and chemist alike.

There is a long history of analyzing chemical and enzyme kinetics using flow techniques.<sup>2–4</sup> These fall into three classes: stopped flow, quenched flow, and continuous flow. It has generally been assumed that the applicability of flow techniques to kinetic analyses requires that the flow of the liquid through the tubing of the instrument be turbulent.<sup>2,3</sup> This ensures there is no radial variation in the flow rate about the central axis of the flow (i.e., there is uniform flow). When this is true, one can calculate the reaction time of a given volume element simply from the total flow rate and the distance traveled from the mixer.

Recently, several papers have appeared that report the successful analysis of protein folding and enzyme kinetics using conditions in which turbulent flow is not achieved.<sup>5–10</sup> Instead, laminar flow prevails, where there is a radial variation of flow rate about the central axis of the flow. Laminar flow, unlike turbulent flow, has the effect of parabolically distorting the flow profile. The success of the reported kinetic analyses under laminar flow conditions and a recent computational analysis of the effect of laminar flow and molecular diffusion on such experiments demonstrates that its presence is not prohibitive to accurate kinetic analyses.<sup>11</sup>

A continuous-flow system that operates under laminar flow conditions is described here. It is a generally applicable system that can be used to analyze both enzymatic and nonenzymatic reactions. The components are commercially available, and it is straightforward to use to generate high precision kinetic data useful in kinetic isotope effect as well as other determinations.

## EXPERIMENTAL SECTION

**Instrumental Setup.** The continuous-flow system is diagrammed in Figure 1. It employs three syringe pumps that were purchased from KD Scientific (New Hope, PA). The two pumps

\* To whom correspondence should be addressed. Phone: 530-754-5282. Fax: 530-752-8995. E-mail: mdtoney@ucdavis.edu.

<sup>†</sup> Current address: Monsanto Company, 800 North Lindbergh Boulevard, St. Louis, MO 63167.

<sup>‡</sup> Current address: National Enzyme Company, 15366 US Hwy 160, Forsyth, MO 65653.

(1) Rosenberg, S.; Kirsch, J. F. *Anal. Chem.* **1979**, *51*, 1379–1383.

(2) Johnson, K. A. *Methods Enzymol.* **1995**, *249*, 38–61.

(3) Hartridge, H.; Roughton, F. J. W. *Proc. R. Soc. (London)* **1923**, *A104*, 376–394.

(4) Gibson, Q. H. *Methods Enzymol.* **1969**, *16*, 187–228.

(5) Zhou, X. Z.; Toney, M. D. *J. Am. Chem. Soc.* **1998**, *120*, 13282–13283.

(6) Zechel, D. L.; Konermann, L.; Withers, S. G.; Douglas, D. J. *Biochemistry* **1998**, *37*, 7664–7669.

(7) Simmons, D. A.; Konermann, L. *Biochemistry* **2002**, *41*, 1906–1914.

(8) Teilum, K.; Maki, K.; Kragelund, B. B.; Poulsen, F. M.; Roder, H. *Proc. Natl. Acad. Sci. U.S.A.* **2002**, *99*, 9807–9812.

(9) Park, S. H.; Shastry, M. C.; Roder, H. *Nat. Struct. Biol.* **1999**, *6*, 943–947.

(10) Kuwata, K.; Shastry, R.; Cheng, H.; Hoshino, M.; Batt, C. A.; Goto, Y.; Roder, H. *Nat. Struct. Biol.* **2001**, *8*, 151–155.

(11) Konermann, L. *J. Phys. Chem.* **1999**, *103*, 7210–7216.

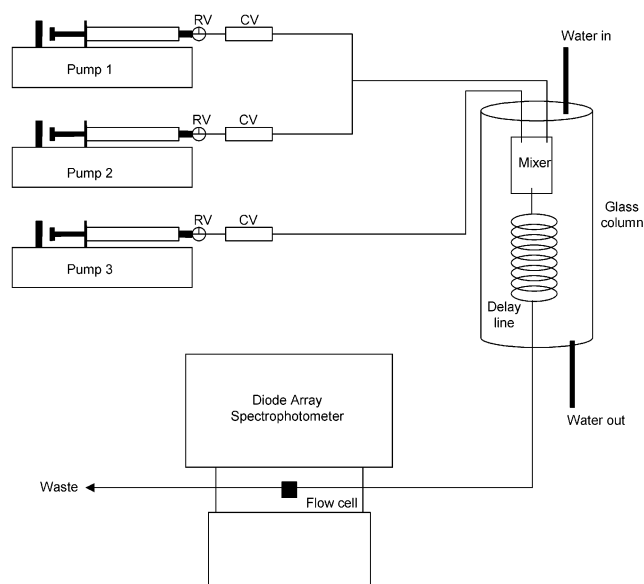


Figure 1. Schematic diagram of the continuous-flow system. Three syringe pumps are shown. Pumps 1 and 2 are programmable pumps that can be used to deliver a linear gradient and are outfitted with 2.5-mL syringes. Pump 3 is not programmable and is outfitted with a 1-mL syringe. The syringes are connected to three-way valves that allow convenient refilling from a reservoir syringe. This feeds into a check valve to prevent backflow. The flow from pumps 1 and 2 meet in a T-junction, which feeds into one side of the mixer. The third pump also feeds into the mixer. The mixer flows into the delay line ( $\sim 300 \mu\text{L}$ ), which flows into the observation cell ( $8\text{-}\mu\text{L}$  volume). The observation cell is placed in a Hewlett-Packard 8453 diode-array spectrophotometer. The mixer and delay line are contained in a glass column through which constant-temperature water is circulated.

used to generate gradients are model 200P programmable pumps capable of delivering linear ramps of flow rate vs time. The two pumps are both connected to a single momentary-contact switch that controls pump start in order to initiate the flow programs simultaneously. The third pump is a model 101. The listed accuracy of the pumps is  $\pm < 1\%$ , and the listed reproducibility is  $\pm 0.1\%$ . The syringes employed are Kloehn series 4000, which give significantly less flow variation than syringes from Hamilton. The gradient pumps were equipped with 2.5-mL syringes, and the third pump, with a 1-mL syringe. The mixer used here is a silicon wafer microvolume multistage static mixer ( $\mu\text{Emu-3}$ ) obtained from Micro-Comp E.v. (Ilmenau, Germany). It consists of a series of 25 microetched mixing elements, each with a volume of  $0.125 \mu\text{L}$  ( $3.1 \mu\text{L}$  total mixer volume). Adapters to connect the mixer to HPLC tubing were also provided by Micro-Comp. The tubing used is 0.02-in. (0.51 mm) i.d. PEEK tubing obtained from Upchurch Scientific. The syringes are connected to three-way valves (Upchurch V100T) useful for refilling from a reservoir syringe, followed by check valves (Upchurch P-790) to prevent reverse flow into the syringes. The two programmable pumps meet at a T-joint, which feeds one side of the mixer input. The second mixer input receives the enzyme (or constant reagent) flow from pump 3. The output of the mixer leads into the delay line ( $\sim 300 \mu\text{L}$ ), where the reaction proceeds. The delay line is connected to a quartz flow cell (Hellma 178.713) with an  $8\text{-}\mu\text{L}$  observation chamber and a path length of 1 cm (1-mm-diameter optical aperture). The flow cell is placed in a Hewlett-Packard 8453 diode array spectrophotometer for detection. Hewlett-Packard software

controls the instrument and data collection. The use of the diode array spectrophotometer allows simultaneous detection of reaction progress as well as dye concentration, which is added for experimental gradient determination when the concentration of a reaction component is ramped linearly. The mixer and delay line are enclosed in a large-diameter glass column that is capped with rubber stoppers. The column is connected to a circulating water bath to maintain constant temperature. A small segment (kept to a minimum) of the delay line is necessarily outside the glass column as it leads to the flow cell.

**Reaction of DTT with DTNB.** The reaction conditions in all cases were 0.1 M potassium acetate pH 4.6,  $25^\circ\text{C}$ . This reaction was first performed manually under pseudo-first-order conditions ( $25 \mu\text{M}$  DTNB, 0.25–4 mM DTT) in cuvettes, following absorbance at 412 nm using a Kontron 9420 spectrophotometer. The time courses were fitted to a single exponential integrated rate equation to obtain the values of  $k_{\text{obs}}$ . These were plotted against DTT concentration, and the slope of the fitted straight line was taken as the value of the second-order rate constant.

A linear gradient ( $80 \mu\text{L}/\text{min}$  constant total flow rate) between buffer (pump 1) and buffer + 5 mM DTT +  $\sim 5 \mu\text{M}$  bromophenol blue (pump 2) was used. The third pump delivered  $250 \mu\text{M}$  of DTNB in buffer at a constant flow rate of  $20 \mu\text{L}/\text{min}$  to give a total combined flow rate for all three pumps of  $100 \mu\text{L}/\text{min}$ . Bromophenol blue absorbs slightly at 412 nm, where the thionitrobenzoate product is followed. The 412-nm data were corrected using the bromophenol blue extinction coefficient ratio for 412 and 595 nm, where bromophenol blue was followed. This was obtained in a separate flow experiment in which DTT and DTNB were left out under otherwise identical conditions. An  $\epsilon_{412} = 13\,600 \text{ M}^{-1}\text{cm}^{-1}$  was used for thionitrobenzoate.

The bromophenol blue 595-nm absorbance trace was used to calculate the concentration of DTT in the reaction flow. Importantly, this provides a direct experimental determination of the concentration of the varied reactant in the flow cell. As in all experiments employing gradients, an initial short trace of 100% pump A and a final short trace of 100% pump B were collected. These yield experimental dye absorbance values that correspond to pure solution A and pure solution B, which can then be used to calculate accurate concentrations of the varied reactant along the gradient, on the basis of the 595-nm absorbance trace.

Flow analysis of this reaction requires knowledge of the exact time between mixing and observation. This was measured by flowing buffer at  $50 \mu\text{L}/\text{min}$  from both of the gradient pumps and injecting a  $4\text{-}\mu\text{L}$  dye pulse into this flow at the mixer using the third pump at  $t_0$ . The time of the peak of the dye pulse was taken as the reaction time. It was found to be  $200 \pm 2 \text{ s}$  from an average of five determinations.

**Tyrosine Phosphatase Kinetic Assays.** The wild-type *Yersinia pestis* protein tyrosine phosphatase was a gift of Professor Z.-Y. Zhang of the Albert Einstein College of Medicine. The enzyme assay employed *p*-nitrophenyl phosphate (PNPP) as substrate under the conditions described by Zhang et al. for pH 6.0.<sup>12</sup> Saturation curves were performed with buffer in syringe 1 and buffer + 12 mM PNPP +  $\sim 5 \mu\text{M}$  methylene blue in syringe 2. The third syringe contained diluted enzyme in buffer. Syringes

(12) Zhang, Z. Y.; Palfey, B. A.; Wu, L.; Zhao, Y. *Biochemistry* **1995**, *34*, 16389–16396.

1 and 2 were flowed complementarily to give a net 80  $\mu\text{L}/\text{min}$  flow rate with a linear gradient between them. The third syringe was flowed at 20  $\mu\text{L}/\text{min}$  to give a total flow rate of 100  $\mu\text{L}/\text{min}$ . The ratio of the extinction coefficients of methylene blue at 660 and 410 nm was determined in separate flow experiments in the absence of substrate and enzyme under otherwise identical conditions. This was used to correct the 410-nm rate data based on the observed 660-nm methylene blue absorbance in flow determinations of kinetic parameters. The 660-nm methylene blue absorbance in the flow experiments was used to calculate the concentration of PNPP in the reaction flow, as described above for the DTNB analysis. The proton inventory experiment was performed under identical conditions, except that both syringes 1 and 2 contained 50 mM PNPP, while syringe 1 contained  $\text{H}_2\text{O}$  and syringe 2 contained  $\text{D}_2\text{O}$  as solvent. The enzyme in syringe 3 was in 50%  $\text{D}_2\text{O}$ .

## RESULTS AND DISCUSSION

**Laminar Flow Considerations.** Traditionally, it has been considered a requirement of continuous-flow or stopped-flow experiments that the flow of the liquid through the instrument tubing be turbulent in nature.<sup>2,3</sup> Turbulent flow is achieved when the Reynolds number of the system is  $>2000$ .<sup>13</sup> High flow rates and large-diameter tubing favor turbulent over laminar flow, but these also increase sample consumption. Turbulent flow is considered to give a uniform flow rate across the entire cross section of the tubing and an effectively undistorted solute propagation profile. Laminar flow takes place when the Reynolds number is  $<2000$ . This type of flow has a radially asymmetric flow profile. The greatest flow rate is along the central axis of the flow, with flow rate decreasing toward zero at the wall of the tubing. This gives a parabolic flow profile.

Recently, several types of kinetics experiments ranging from fluorescence detection of protein folding to electrospray ionization mass spectrometry detection of transient enzymatic reaction intermediates to steady-state enzyme kinetics have been successfully performed under laminar flow conditions in widely differing time regimes.<sup>5–10</sup> Thus, turbulent flow is not an absolute requirement for successful flow kinetics experiments.

Taylor gave the first theoretical treatment of flow under laminar conditions.<sup>14</sup> He showed that molecular diffusion plays a remarkable role in the solute concentration distribution in a laminar flow. In the absence of diffusion, solute from an initial thin plug is distributed over a large length of tubing. The diffusion of solute radially across the tubing cross section continuously moves solute from slowly to quickly moving flow elements, and vice versa. For an initial thin plug of solute, this has the extraordinary effect of generating a symmetric concentration profile centered at the average flow velocity after a sufficiently long time, as illustrated in Figure 2.

Taylor derived the time required for the radial variation in a solute concentration to die down to  $1/e$  of its initial value,

$$t_1 = r^2/14.4D \quad (1)$$

where  $r$  is the radius of the tubing and  $D$  is the molecular diffusion

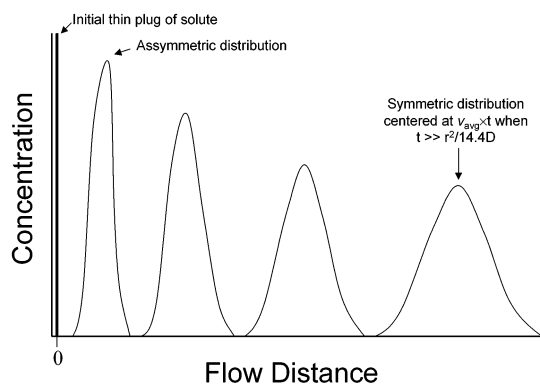


Figure 2. Symmetrization of the concentration profile from an initial thin plug of solute. Taylor showed that an initial thin plug of solute in a laminar flow first forms an asymmetric distribution that, after a defined period, becomes symmetrized as a result of the action of molecular diffusion. Continuous-flow kinetics experiments require that the time of the reaction flow be long enough for symmetrization to occur.

coefficient. When the duration of the flow is much longer than this time, a symmetric concentration profile is obtained with the peak of the profile centered at  $v_{\text{avg}}t$  along the tubing. Concentration profile symmetrization from diffusive averaging of the flow velocities of solute molecules is facilitated when the flow is slow, when the radius of the tubing is small, and when the molecular diffusion coefficient is large. Konermann analyzed computationally the effects of laminar flow on kinetics experiments and reached the conclusion that “the distortion of the measured kinetics under laminar flow conditions is surprisingly small, especially when the reaction occurs on a time scale at which molecular diffusion in the tube has notable effects on the age distribution function”.<sup>11</sup>

The Reynolds number calculated for the present system is 4.7, much less than 2000. Thus, laminar flow conditions prevail. Although a symmetric (or nearly so) solute concentration profile is necessary, the most important requirement for kinetic studies is that the peak of the concentration profile from an initial thin plug flows through the observation cell after a volume of flow equal to the volume of the tubing between the mixer and the observation cell (i.e., the profile peak passes through the observation cell after delay line volume/average flow rate). In this case, the time of passage of the peak through the observation cell can be reasonably associated with the reaction time of an initial thin plug of reactants that gives rise to the peak.

In the present system, a linear concentration gradient of one reactant is mixed with a constant concentration of another. The fluid exiting the mixer thus consists of a continuous series of infinitesimally thin plugs of reactants that differ in the concentration of one reactant. If the time of flow between the mixer and observation cell is much greater than  $t_1$ , then what is observed in the cell as a function of time is a series of overlapping symmetric concentration profiles that differ by infinitesimally small time separations. The result is that the reactant (or product) concentration observed at any given time in the cell is a boxcar average, the effective width of which is determined by the volume of the observation cell and the total volume of the gradient. Here, the observation cell has a volume of 8  $\mu\text{L}$ , and the total gradient volumes are  $\sim 4000 \mu\text{L}$ .

(13) Steinfeld, J. I.; Francisco, J. S.; Hase, W. L. *Chemical Kinetics and Dynamics*, 2nd ed.; Prentice Hall: Upper Saddle River, NJ, 1999.

(14) Taylor, G. *Proc. R. Soc. (London)* **1953**, A219, 186–203.

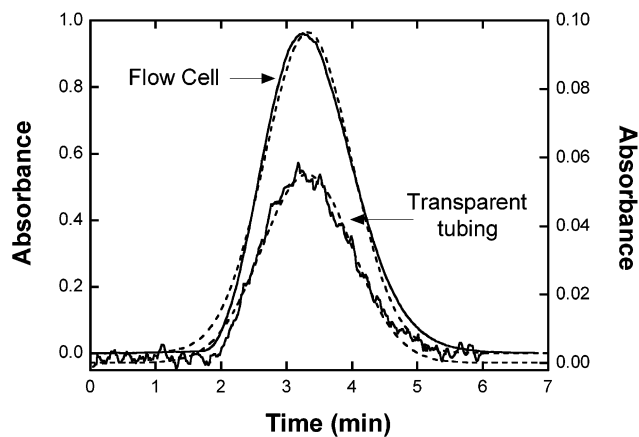


Figure 3. Observed concentration profiles for a 4- $\mu\text{L}$  dye pulse injected into a 100  $\mu\text{L}/\text{min}$  flow. The larger peak with less noise was observed using the 8- $\mu\text{L}$  quartz flow cell. The smaller peak with more noise was observed by replacing the flow cell with 0.51-mm-i.d. transparent tubing. The dashed lines are fits to eq 28 from Taylor, which describes solute distribution after symmetrization.<sup>14</sup>

**Performance of the System.** The system described here differs in important ways from that described previously.<sup>5</sup> The mixer used in the previous system was home-built. It employed a magnetic stir bar in a mixing chamber that directly received all three solutions to be mixed. The magnetic stir bar required that a stir plate be placed directly under the mixer when it was in the glass column flow chamber used to maintain constant temperature. The practical problems associated with that design included the trapping of bubbles that were difficult to remove from the mixing chamber and the loss of magnetic connection between the stir plate and the stir bar in the mixing chamber. The present mixer is not an active one as used previously; rather, it is a passive one with multiple (25) mixing stages, each with a very small volume (0.125  $\mu\text{L}$ ). This eliminates the practical issues described above and provides more homogeneous mixing as gleaned from the higher stability of absorbance traces for dye solutions of constant composition (data not shown).

The second major design improvement involves the use of the diode-array spectrophotometer with the microvolume flow cell. The previous design employed two HPLC absorbance detectors in series. Thus, there was a time delay between the observation of the reaction progress (substrate or product concentration) and the position of the gradient (dye). A somewhat subjective correction for this delay time had to be applied to the data, opening the possibility for error. This is avoided with the diode-array spectrophotometer, since the reaction progress and position of the gradient are measured simultaneously from a single flow cell with the multichannel detector. The microvolume (8- $\mu\text{L}$ ) flow cell provides a fine sampling of the gradient without compromising flow properties.

The symmetrization of a thin plug of solute was tested with the present system under typical reaction conditions by injecting a small volume of concentrated methylene blue dye into a flow of water. Figure 4 shows the observed concentration profile when 3  $\mu\text{L}$  of methylene blue (20  $\mu\text{L}/\text{min}$ ) is injected into a 100  $\mu\text{L}/\text{min}$  flow of water. The profile is nearly symmetrical, and the peak is observed at a volume corresponding to that calculated on the basis of the tubing length and the diameter reported by the manufacturer. The diameter of the observation cell is twice that of the

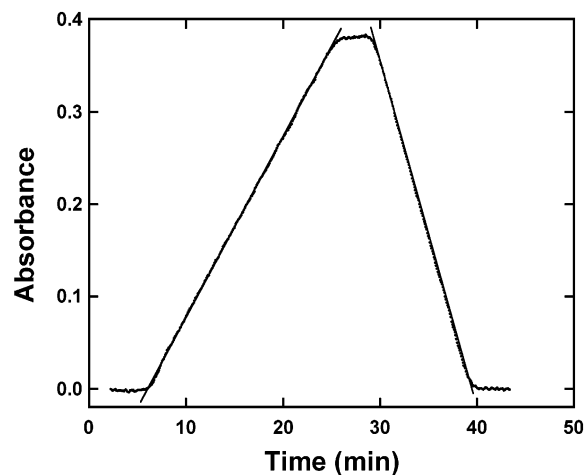


Figure 4. Linearity of gradients formed by the system. A linear gradient of dye was programmed to demonstrate that both steep and shallow gradients are highly linear.

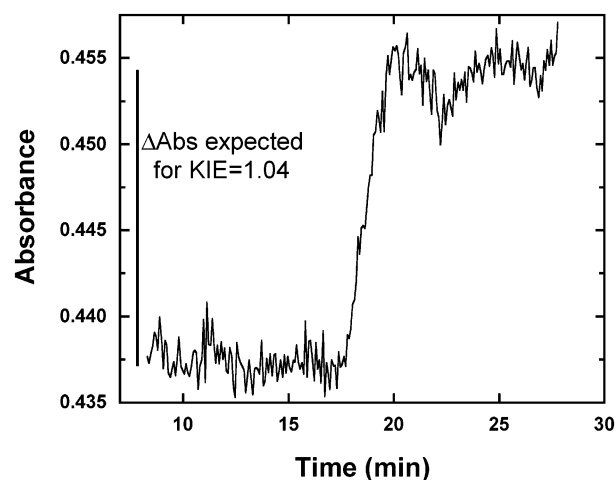


Figure 5. KIE determination simulated with dye. An increase in dye concentration corresponding to a KIE of 1.04 was programmed. The source of the noise in this type of experiment likely comes from the small (1-mm)-diameter aperture of the flow cell and the unfocused, relatively weak beam of the spectrophotometer.

delay line tubing, which could potentially pose problems. This was tested by using transparent tubing (0.51-mm i.d.) as the observation cell by placing it directly in the spectrophotometer beam. The profile observed (Figure 3) is essentially identical to that using the quartz flow cell, eliminating the flow cell diameter as a potential source of problems.

Several applications of this system (e.g., saturation curves for enzymes, proton inventories) require a linear gradient between two solutions. The linearity of the gradient formed by complementarily programming the flow of pumps 1 and 2 at a constant total flow rate was examined by forming a methylene blue dye gradient. This is shown in Figure 4. As can be seen, the system provides extremely linear gradients in both shallow and steep transitions.

A preliminary report demonstrated the applicability of this system to the determination of heavy atom kinetic isotope effects (KIEs) in an enzymatic reaction.<sup>5</sup> Figure 5 shows the performance of the current setup (which differs from that in the preliminary report) in such an application, as simulated with dye. The ratio of buffer to buffer + dye was changed in this experiment to simulate

a KIE of 1.04. Such an effect is clearly measurable with precision, and given the noise level, perhaps a quarter of this value would be statistically significant. The observed change in absorbance due to heavy-atom substitution depends linearly on the absolute absorbance change, and thus, the precision of KIE measurements can be enhanced by optimizing the reaction conditions to give large absorbance changes with the natural abundance substrate before making the isotopic comparison. Another likely source of the noise seen in Figure 5 is the small (1-mm) aperture of the flow cell and the relatively low intensity unfocused beam of the diode-array spectrophotometer. A larger aperture is not desired, because this would increase the volume of the flow cell, but increasing the amount of light passing through the cell would probably improve noise dramatically.

A KIE experiment is performed here by alternating between pumps containing substrates with light and heavy isotopes, measuring the change in absorbance due to heavy atom substitution. This necessarily requires a fixed substrate concentration that is identical for the light and heavy isotope containing solutions. Thus, kinetic isotope effects on  $k_{\text{cat}}$  are technically easy to measure using substrate concentrations that are much greater than  $K_M$ . Under these conditions, variation in substrate concentration between light and heavy isotopes has a minimal effect. Kinetic isotope effects under nonsaturating conditions are technically more difficult. The rate observed at low substrate concentrations (i.e., less than  $K_M$ ) is linearly dependent on concentration. Therefore, errors in substrate concentration propagate linearly into KIEs measured under nonsaturating conditions, which may be limited by this factor.

The KIEs measured at partially saturating substrate concentrations are a combination of those on  $k_{\text{cat}}$  and  $k_{\text{cat}}/K_M$ . The latter kinetic parameter governs the rate of reaction between the free enzyme and free substrate, while the former governs the rate of reaction of the enzyme–substrate complex.<sup>15</sup> Thus, the fraction of the enzyme that is substrate-bound will yield the KIE on  $k_{\text{cat}}$ , and the fraction of the enzyme that is free will yield the KIE on  $k_{\text{cat}}/K_M$ . The true value of the KIE on  $k_{\text{cat}}/K_M$  is obtained intrinsically from competitive experiments in which both isotopically labeled substrates are present in a single reaction mixture. Such experiments are typically performed with radioactively labeled substrates or with stable isotopes and an isotope ratio mass spectrometer.<sup>16</sup> It is proposed here that the best method for obtaining the true KIEs on both  $k_{\text{cat}}$  and  $k_{\text{cat}}/K_M$  is to measure the KIE at multiple values of fractional enzyme saturation by substrate. The true values of the KIEs would be obtained from extrapolations of the observed KIEs to zero fractional saturation for  $k_{\text{cat}}/K_M$  and a fractional saturation of 1 for  $k_{\text{cat}}$ .

**Reaction of DTT with DTNB.** The flow system described here is not limited to the analysis of enzyme-catalyzed reactions. In principle, any type of kinetic process in which high precision is required can be analyzed with appropriate adjustments in the delay lines, etc. As an example, we chose to study the reaction of DTT with DTNB under pseudo-first-order conditions. In this reaction, the two thiols of DTT are oxidized in a disulfide exchange reaction with DTNB to give two molecules of thionitrobenzoate, which absorb strongly at 412 nm. A comparison of the rate constant

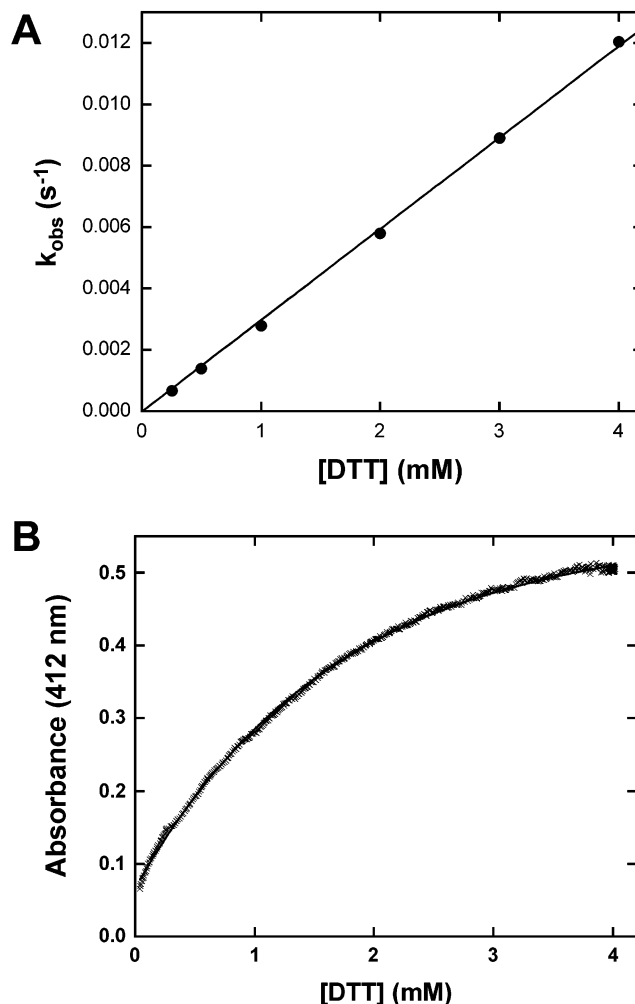


Figure 6. (A) Manual determination of the second-order rate constant for the reaction of DTT with DTNB at pH 4.6 and 25 °C. The slope of the plot is taken as the rate constant, which is  $3.0 \pm 0.1 \text{ M}^{-1} \text{ s}^{-1}$ . (B) Continuous-flow determination of the same second-order rate constant for the reaction of DTT with DTNB. The line is from a fit to eq 5 written in terms of thionitrobenzoate concentration. The value of the rate constant obtained from an average of five such determinations is  $2.93 \pm 0.08 \text{ M}^{-1} \text{ s}^{-1}$ .

obtained from a traditional analysis and that obtained from the flow system provides a direct test of the performance of the flow system.

This simple reaction can be analyzed readily by the traditional method using cuvettes and manually mixed reactions under pseudo-first-order conditions. The data obtained are shown in Figure 6A. They give a second-order rate constant of  $3.0 \pm 0.1 \text{ M}^{-1} \text{ s}^{-1}$  from the six reactions.

The analysis of the pseudo-first-order reaction by continuous flow is straightforward but somewhat different from the manual method. The general mechanism is



When  $[\text{DTT}_{\text{red}}] \gg [\text{DTNB}]$ , the rate equation can be written as

$$-\frac{d[\text{DTNB}]}{dt} = k[\text{DTT}_{\text{red}}][\text{DTNB}] = k'[\text{DTNB}] \quad (3)$$

(15) Fersht, A. *Structure and Mechanism in Protein Science: A Guide to Enzyme Catalysis and Protein Folding*, W. H. Freeman: New York, 1999.

(16) O'Leary, M. H. *Methods Enzymol.* **1980**, *64*, 83–104.

where  $K = k[\text{DTT}_{\text{red}}]$ . This can be integrated to give the time dependence of  $[\text{DTNB}]$  as follows

$$[\text{DTNB}]_{(t, [\text{DTT}_{\text{red}}])} = [\text{DTNB}]_0 e^{-Kt} = [\text{DTNB}]_0 e^{-k[\text{DTT}_{\text{red}}]t} \quad (4)$$

Here, the reaction time is a constant, and the concentration of DTT is varied linearly in the flow system. Thus, the reaction course takes the form

$$[\text{DTNB}]_{([\text{DTT}_{\text{red}}])} = [\text{DTNB}]_0 e^{-K'([\text{DTT}_{\text{red}}])} \quad (5)$$

where  $K' = kt$ . This shows that the concentration of DTNB will decrease exponentially with increasing  $[\text{DTT}_{\text{red}}]$  (and conversely, that the concentration of thionitrobenzoate will increase exponentially with increasing  $[\text{DTT}_{\text{red}}]$ ).

The prediction of eq 5 that the thionitrobenzoate concentration will increase exponentially with  $[\text{DTT}_{\text{red}}]$  is borne out by experiment, as shown in Figure 6B. The determination of the rate constant from the continuous-flow data requires the knowledge of  $t$ , the time of reaction. This was obtained from dye-pulse experiments and was found to be  $200 \pm 2$  s from an average of five determinations. Using this value of  $t$ , the continuous-flow analysis gave a value of  $2.93 \pm 0.08 \text{ M}^{-1} \text{ s}^{-1}$  obtained from an average of five runs. This is in remarkable agreement with the value obtained by the manual analysis and validates the general kinetic utility of the flow system as described.

The flow system could, in principle, be used to analyze true first-order reactions. In this case, the reaction time requires variation. A general strategy would be to vary the reaction time by varying the total flow rate. The reaction might be initiated in the mixer by, for example, a pH change, and the total flow rate would be decreased or increased linearly. One would have to ensure that, at the highest flow rate, a dye pulse becomes a symmetrized peak before entering the observation cell.

**Analysis of the Tyrosine Phosphatase-Catalyzed Hydrolysis of *p*-Nitrophenyl Phosphate.** The tyrosine phosphatase from *Y. pestis* is a virulence-determining factor that functions by dephosphorylating host proteins and thereby disturbing metabolic control.<sup>17,18</sup> This enzyme can hydrolyze a variety of phosphate esters, and PNPP is one of the best substrates.<sup>19</sup>

The tyrosine phosphatase-catalyzed hydrolysis of PNPP was chosen as an enzymatic test case for the flow system. Zhang et al. reported the kinetic parameters for this reaction at pH 6.0.<sup>12</sup> The flow system was used under initial rate conditions, performing a linear gradient of  $[\text{PNPP}]$  with time. Thus, the absorbance values observed represent single time point initial rate determinations of the enzymatic reaction. Given the initial rate conditions, the data should conform to the Michaelis–Menten equation cast in its usual form.

The dye methylene blue was added to the PNPP solution, and the 660-nm absorbance from the dye was used to calculate the  $[\text{PNPP}]$  corresponding to the observed 410-nm (*p*-nitrophenol)

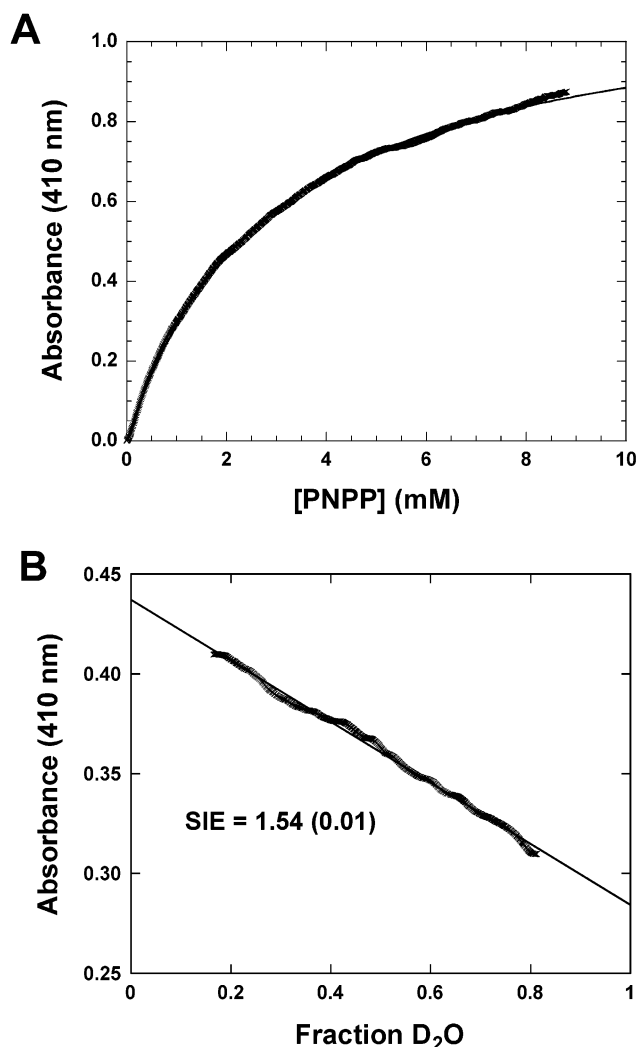


Figure 7. (A) Saturation curve for the *Y. pestis* protein tyrosine phosphatase using PNPP as substrate at pH 6.0. The line is from a fit to the Michaelis–Menten equation. The data reproduce the kinetic parameters reported previously.<sup>12</sup> (B) Proton inventory on  $k_{\text{cat}}$  for the phosphatase. The linearity of the data indicate a single proton in flight in the transition state. The observed solvent isotope effect (SIE) of 1.54 is in close agreement with that reported previously.<sup>19</sup>

data. A typical set of absorbance (i.e., initial rate) data are plotted against the calculated  $[\text{PNPP}]$  data in Figure 7A. The line fitted through the data is that for the Michaelis–Menten equation. The flow data faithfully reproduce the previously reported kinetic parameters.<sup>12</sup> For example, a  $K_M$  value of 2.6 mM (without an associated error) was reported, and the flow analysis gives a value of  $2.5 \pm 0.2$  mM.

Another potentially very important application of the flow system is for the determination of high precision proton inventories. In this type of experiment, the atom fraction of deuterium in the solvent is varied, and the rate of the reaction is monitored. Plots of deuterium content vs reaction rate are mechanistically informative, since the number of protons in flight in the rate-determining step corresponds to the order of the polynomial required to fit the data best. The well-known Gross-Butler equation describes this behavior.<sup>20</sup>

A proton inventory for the *Y. pestis* tyrosine phosphatase has not yet been reported. One has been reported by Zhang and Van

(17) Bliska, J. B.; Guan, K. L.; Dixon, J. E.; Falkow, S. *Proc. Natl. Acad. Sci. U.S.A.* **1991**, *88*, 1187–1191.

(18) Guan, K. L.; Dixon, J. E. *Science* **1990**, *249*, 553–556.

(19) Zhang, Z. Y.; Malachowski, W. P.; Van Eetten, R. L.; Dixon, J. E. *J. Biol. Chem.* **1994**, *269*, 8140–8145.

Etten for  $k_{\text{cat}}$  with the bovine enzyme and 4-phenylbutyl phosphate as substrate.<sup>21</sup> In that case, phosphorylation of the enzyme was shown to be the rate determining step, and the proton inventory was linear, indicating a single proton in flight in the transition state. On the other hand, burst kinetics and other data clearly show that dephosphorylation of the phosphoenzyme intermediate is the rate-determining step for  $k_{\text{cat}}$  with the *Y. pestis* enzyme reacting with PNPP.<sup>12</sup>

A proton inventory on  $k_{\text{cat}}$  for the phosphatase obtained in a continuous-flow experiment is shown in Figure 7B. The data are linear and consistent with a single proton in flight in the phosphoenzyme hydrolysis transition state. This is expected to be the proton donated by Asp356 to the Cys403 thiolate leaving group in the dephosphorylation step.<sup>19</sup> The KIE value obtained from this experiment ( $1.54 \pm 0.01$ ) is in close agreement with the solvent KIE previously reported (1.5, no error given).<sup>19</sup>

**Other Potential Applications.** The flow system described here is a general purpose kinetic analysis system that is useful for reactions that occur on the time scale of approximately a minute or more. The applicable time scale could potentially be reduced by decreasing the tubing diameter, which would allow peak symmetrization in a shorter time. Roder has, in fact, described a purpose-designed flow system operating under laminar flow conditions that is capable of measuring fast reactions with a dead time of  $\sim 50 \mu\text{s}$ .<sup>22</sup> He has applied this system to the fluorescence monitoring of protein folding.<sup>8–10</sup> In principle, there is no limit to the reduction of the volume of the system, since

laminar flow conditions will continue to prevail as the volume is reduced. There are already examples of microfluidic “lab-on-a-chip” devices that perform enzyme kinetic analyses with nanoliter volumes.<sup>23</sup>

The technique of stopped-flow injection analysis has been applied to the determination of rate constants in both nonenzymatic and enzymatic reactions.<sup>24,25</sup> The present system could reproduce this type of analysis by stepping between discrete concentrations of the varied reactant, each time stopping the flow and observing the time dependence of the reaction. In addition, one could add a dye to determine experimentally the concentration of the varied reactant.

An important potential application of the system described here is for the conversion of discontinuous spectrophotometric kinetic assays into continuous ones. One could imagine, for example, continuously determining the concentration of a remaining thiol substrate in an enzymatic reaction by adding a second mixer after the delay line and combining the reaction flow with a DTNB flow from a fourth pump. This second mixer would then feed into the flow cell, and thionitrobenzoate absorbance monitored continuously.

A further potential application of this flow system is to the determination of pH rate profiles. Substrate would be placed in a multicomponent buffer at, for example, low pH in syringe 1 and at high pH in syringe 2. A gradient between these would give a pH variation that might be monitored either by a flow-through pH electrode or spectrophotometrically by a combination of indicator dyes included in the reaction flow.

(20) Cook, P. F. *Enzyme Mechanism from Isotope Effects*; CRC Press: Boca Raton, FL, 1991.

(21) Zhang, Z. Y.; Van Etten, R. L. *Biochemistry* **1991**, *30*, 8954–8959.

(22) Shastry, M. C.; Luck, S. D.; Roder, H. *Biophys. J.* **1998**, *74*, 2714–2721.

(23) Wang, J. *Electrophoresis* **2002**, *23*, 713–718.

(24) Hungerford, J. M.; Christian, G. D.; Ruzicka, J.; Giddings, J. C. *Anal. Chem.* **1985**, *57*, 1794–1798.

(25) Crouch, S. R.; Cullen, T. F.; Scheeline, A.; Kirkor, E. S. *Anal. Chem.* **1998**, *70*, 53–106.

#### ACKNOWLEDGMENT

This work was supported by NIH grant GM54779 to MDT.

Received for review January 24, 2003. Accepted April 24, 2003.

AC034068J